Microbiome Determinants and Physiological Effects of the Benzoate-Hippurate Microbial-Host Co-Metabolic Pathway — Source link ↗

Francois Brial, Julien Chilloux, Trine Nielsen, Sara Vieira-Silva ...+23 more authors

Institutions: University of Paris, Imperial College London, University of Copenhagen, Nottingham Trent University ...+6 more institutions

Related papers:

- Stability and Robustness of Human Metabolic Phenotypes in Response to Sequential Food Challenges

- Dynamic metabonomic and microbiological response of rats to lincomycin exposure: an integrated microbiology and metabonomics analysis

- Integrative metagenomic and metabolomic analyses reveal severity-specific signatures of gut microbiota in chronic kidney disease

- An integrated metabonomic approach to studying metabolic profiles in rat models with insulin resistance induced by high fructose

- 1H NMR-based metabonomic analysis of serum and urine in a nonhuman primate model of diabetic nephropathy.

1 **Microbiome Determinants and Physiological Effects of the Benzoate-Hippurate**

2 **Microbial-Host Co-Metabolic Pathway**

3

4 François Brial[1,17], Julien Chilloux[2,17], Trine Nielsen[3,17], Sara Vieira-Silva[4,5,17], Gwen Falony[4,5],

5 Lesley Hoyles[2,6], Ana L. Neves[2], Andrea Rodriguez-Martinez[2], Ghiwa Ishac Mouawad[1],

6 Nicolas Pons[7], Sofia Forslund[8,9], Emmanuelle Le Chatelier[7], Aurélie M. Le Lay[1], Jeremy K

7 Nicholson[2], Torben Hansen[3], MetaHIT consortium, Karine Clément[11,12], Peer Bork[7,13], S.

8 Dusko Ehrlich[14,15], Jeroen Raes[4,5,18], Oluf Pedersen[3,18], Dominique Gauguier[1,2,16,18], Marc-

9 Emmanuel Dumas[2,16,18]

10

11 [1] Université de Paris, INSERM UMRS 1124, 45 rue des Saints Pères,75006 Paris, France.

12 [2]Imperial College London, Division of Computational and Systems Medicine, Dept of Surgery

13 and Cancer, Faculty of Medicine, Sir Alexander Fleming building, Exhibition Road, South

14 Kensington, London SW7 2AZ, UK.

15 [3] The Novo Nordisk Foundation Center for Basic Metabolic Research, Faculty of Health and

16 Medical Sciences, University of Copenhagen, DK-2200 Copenhagen, Denmark.

17 [4]Laboratory of Molecular Bacteriology, Department of Microbiology and Immunology, Rega

18 Institute, KU Leuven, Herestraat 49, B-3000 Leuven, Belgium.

19 [5]Center for Microbiology, VIB, Kasteelpark Arenberg 31, B-3000 Leuven, Belgium.

20 [6]Nottingham Trent University, Department of Biosciences, School of Science and

21 Technology, Clifton, Nottingham NG11 8NS, UK.

22 [6]Nottingham Trent University, Department of Biosciences, School of Science and

23 Technology, Clifton, Nottingham NG11 8NS, UK.

24 [7]MGP MetaGénoPolis, INRA, Université Paris-Saclay, 78350 Jouy en Josas, France.

25 [8] Structural and Computational Biology Unit, European Molecular Biology Laboratory, 69117

26 Heidelberg, Germany.

27 [9]Max Delbrück Centre for Molecular Medicine, Berlin, Germany.

28 [10]Experimental and Clinical Research Center, a joint operation of the Max Delbrück Center

29 in the Helmholtz Association and the Charité University Hospital, Berlin, Germany

30 [11]INSERM, U1166, team 6 Nutriomique, Université Pierre et Marie Curie-Paris 6, Paris,

31 France.

32 [12]Institute of Cardiometabolism and Nutrition (ICAN), Assistance Publique-Hôpitaux de

33 Paris, Pitié-Salpêtrière Hospital, Nutrition Department, Paris, France.

34 [13]Department of Bioinformatic Biocentrum, Würzburg University, 97074 Würzburg, Germany

35 [14]Institut National de la Recherche Agronomique, 78350 Jouy en Josas, France.

36 [15]Centre for Host-Microbiome Interactions, Dental Institute Central Office, King's College

37 London, Guy's Hospital, London, UK.

38 [16]McGill University and Genome Quebec Innovation Centre, 740 Doctor Penfield Avenue,

39 Montréal, QC, H3A 0G1, Canada.

40 [17]Co-first authors.

41 [18]Senior authors.

42 Correspondence should be addressed to M.-E.D. m.dumas@imperial.ac.uk or

43 D.G.dominique.gauguier@inserm.fr

44

ABSTRACT

46

Objective. Gut microbial products are involved in type 2 diabetes, obesity and insulin resistance. In particular, hippurate, a hepatic phase 2 conjugation product of microbial benzoate metabolism, has been associated with a healthy phenotype. This study aims to identify metagenomic determinants and test protective effects of hippurate.

51

Design. We profiled the urine metabolome by ^{1}H Nuclear Magnetic Resonance (NMR) spectroscopy to derive associations with metagenomic sequences in 271 middle-aged Danish individuals to identify dietary patterns in which urine hippurate levels were associated with health benefits. We follow up with benzoate and hippurate infusion in mice to demonstrate causality on clinical phenotypes.

57

Results. In-depth analysis identifies that the urine hippurate concentration is associated with microbial gene richness, microbial functional redundancy as well as functional modules for microbial benzoate biosynthetic pathways across several enterotypes. Through dietary stratification, we identify a subset of study participants consuming a diet rich in saturated fat in which urine hippurate, independently of gene richness, accounts for links with metabolic health that we previously associated with gene richness. We then demonstrate causality *in vivo* through chronic subcutaneous infusions of hippurate or benzoate (20 nmol/day) resulting in improved glycemic control in mice fed a high-fat diet. Hippurate improved insulin secretion through increased β-cell mass and reduced liver inflammation and fibrosis, whereas benzoate treatment resulted in liver inflammation.

68

Conclusion. Our translational study shows that the benzoate-hippurate pathway brings a range of metabolic improvements in the context of high-fat diets, highlighting the potential of hippurate as a mediator of metabolic health.

72

73

74

INTRODUCTION

76

The human obesity epidemic raises the risk of type 2 diabetes and cardiovascular disease. Dysbiosis of the gut microbiome is now recognised as a key feature of these disorders.[1] The microbiome collectively encodes up to 10 million different microbial genes.[2,3] In particular, gene richness has been proposed as a marker of ecological diversity mirroring improvements in metabolic health.[4,5] Although the microbiome directly impacts various biological processes of the host through production or degradation of a multitude of compounds, the vast majority of molecules involved in this chemical crosstalk remains elusive.[6-9]

There is growing evidence that hippurate, one of the most abundant microbial-host co-metabolites in human urine, is positively associated with metabolic health through inverse associations with blood pressure, fatty liver disease, visceral fat mass and Crohn's disease.[10-14] Its microbial precursor, benzoate is taken up by organic anion transporter MCT2[15] and conjugated with glycine in the liver and kidney to form hippurate. We showed in a genetic cross between diabetic and normoglycemic rat strains that serum benzoate under host genome control.[16] Hippurate was recently shown to be associated both with microbiota diversity based on 16S rRNA gene sequencing[17] and with reduced risk of metabolic syndrome.[13]

However, there is a critical need for an in-depth characterization of the complex nutrition-microbiome-host interaction in the benzoate-hippurate pathway, in relation to: i) associations with enterotype, gene richness and functional redundancy, ii) population stratification according to nutritional patterns to identify patient sub-groups in which hippurate improves metabolic health, and iii) translational elucidation of these effects on host phenotypes *in vivo*. To address these specific points, we characterized the urinary metabolome and the fecal microbiome of 271 middle-aged non-diabetic Danish individuals from the MetaHIT study.[4] Through dietary stratification we delineate the complex interaction between dietary intake, microbiome and metabolome its impact on body weight, immune and metabolic markers, which we further confirm and characterise in a mouse model of diet-induced obesity and diabetes.

105

106   **METHODS**

107

108   **Human subjects**

109   All analyses were done on non-diabetic Danish individuals from the MetaHIT study

110   (n=271),[4,18] including the subset of 193 individuals who completed a validated food

111   frequency questionnaire (FFQ).[19] The study was approved by the Ethical Committees of

112   the Capital Region of Denmark (HC-2008-017 and H-15000306) and was in accordance with

113   the principles of the Declaration of Helsinki. All individuals gave written informed consent

114   before participating in the study. Sampling and clinical phenotyping were performed as

115   described previously.[4,18] In short, all study participants were recruited from the population-

116   based Inter99 study.[20]. The study program consisted of two visits with approximately 14

117   days apart. At the first visit all participants were examined in the morning after an overnight

118   fast. Blood sampling was performed at the fasting state, and urine was collected upon arrival

119   at the centre. At the second visit, a Dual Energy X-Ray Absorptiometry (DXA) scan was

120   performed. Serum glycine levels were previously assessed.[19] Estimated glomerular

121   filtration rate (eGFR) was calculated with the CKD-EPI formula with age, gender and

122   creatinine (μmol/L) and without ethnicity factor.[21]

123   **Dietary assessment**

124   A subset of the study participants (n=193) completed a validated FFQ in order to obtain

125   information on their habitual dietary habits.[22] The FFQ gathered dietary information from

126   all meals during a day and the intake frequencies within the past months were recorded. The

127   dietary data were evaluated by determining the consumed quantity and multiplying the

128   portion size by the corresponding consumption frequency as reported in the FFQ. Standard

129   portion sizes for women and men, separately, were used in this calculation; all food items in

130   the FFQ were linked to food items in the Danish Food Composition Databank as previously

131   described.[19]. Estimation of daily intake of macro-and micronutrients for each participant

132   was based on calculations in the software program FoodCalc version1.3

133   (http://www.ibt.ku.dk/jesper/FoodCalc/Default.htm).

134   **Sample collection**

135   Fecal sample collection and analysys was performed as previously described.[4] Urine was

136   collected at the first visit upon arrival at the study site and stored at -80°C until analysis.

137   **Metabolic profiling**

138   Urine samples were randomized, prepared and measured on a NMR spectrometer (Bruker)

139   operating at 600.22 MHz ^{1}H frequency using previously published experimental

140   parameters[23] The ^{1}H NMR spectra were then pre-processed and analyzed as previously

141   reported[10] using Statistical Recoupling of Variables-algorithm.[24] Structural assignment

142   was performed as reviewed in [25], using in-house and publicly available databases.

143   **Metagenomics**

144   Shotgun sequencing of microbial DNA and metagenomics processing workflow for gene

145   richness was performed as previously published.[4] Sequences were mapped onto the

146   previously released integrated gene catalog.[2] Following the previously published

147   strategy,[26] we built a novel set of manually curated gut-specific metabolic modules

148   (GMMs) to describe and map microbial phenylpropanoid metabolism from shotgun

149   metagenomic data. The set of 20 modules, following KEGG syntax, is provided in

150   supplement, including references to the original publications where pathways were

151   discovered and described (***Supplementary List***).

152   **Univariate statistical analysis**

153   A ROUT test was performed to identify potential outliers (Q=1%). For statistical comparisons

154   between study groups, normality was tested using D'Agostino-Pearson omnibus normality

155   test, then one-way ANOVA was used, followed by Tukey's HSD post hoc testing when data

156   were normally distributed, otherwise groups were compared using the two-tailed Mann-

157   Whitney test. Data are displayed as mean ± s.e.m in all figures. Multiple testing corrections

158   were performed using Storey's procedure.[27]

159   **Multivariate statistics**

160   Probabilistic principal component analysis (PCA) was performed using MATLAB R2014a

161   function 'ppca' to handle missing values. Unconstrained ordination was performed using

162   principal coordinates analysis (PCoA) to visualize inter-individual variation in microbiota

163   composition using Bray-Curtis dissimilarity on the genus-level abundance matrix using the R

164   package *vegan*.[28] Distance based Redundancy Analysis (dbRDA) was used to determine

165   the cumulative contributions of a matrix of explanatory variables on the response data,

166   hippurate excretion inter-individual variation (Euclidian distance on log-transformed urine

167   hippurate concentration matrix) in R package *vegan*.[28]. Orthogonal partial least squares

168   discriminant analysis (O-PLS-DA) was performed in MATLAB R2014a for supervised

169   multivariate analysis as previously described.[29] The predictive capability of O-PLS-DA

170   models was evaluated through 7-fold cross-validation[29] to compute Q^2_{Yhat} goodness-of-

171   prediction parameters. The empirical significance of the Q^2_{Yhat} parameter was evaluated by

172   random permutation testing (10,000 iterations).[30]

173   **Animal experiments**

174   Six-week-old C57BL/6J male mice (Janvier Labs, Courtaboeuf, France) were maintained in

175   specific pathogen free condition on a 12h light/dark cycle and fed a standard chow diet

6

176   (R04-40, Safe, Augy, France) for a week. Groups of 10 randomly selected mice were then

177   fed either control chow diet (CHD) (D 12450Ki, Research diets, NJ) or high fat (60% fat and

178   sucrose) diet (HFD) (D12492i, Research diets, NJ). One week later, osmotic minipumps

179   (Alzet® model 2006, Charles River Lab France, l'Arbresle, France) filled with a solution of

180   either hippuric acid or benzoic acid (5.55mM in 0.9% NaCl) (Sigma Aldrich, St Quentin,

181   France) were inserted subcutaneously under isoflurane anesthesia. The metabolites were

182   delivered at a rate of 0.15 μL/hour over a 42-day period (20 nmol/day).

183   Glycemia and body weight were recorded weekly. After 3 weeks of metabolite treatment,

184   mice underwent an intra-peritoneal glucose tolerance test (IPGTT, 2g/kg). Blood was

185   collected from the tail vein before glucose injection and 15, 30, 60 and 120 minutes

186   afterwards to determine glycemia using an Accu-Check® Performa (Roche Diagnostics,

187   Meylan, France). Cumulative glycemia (AUC) was calculated as the sum of plasma glucose

188   values during the IPGTT and cumulative glucose increase (ΔG) parameter was calculated

189   as AUC above the fasting glycemia baseline integrated over the 120 min of the IPGTT.

190   Insulinemia was determined at baseline and at 30 minutes using insulin ELISA kits

191   (Mercodia, Uppsala, Sweden). After 6 weeks of metabolite infusion, mice were killed by

192   decapitation and organs were dissected and weighed. Triglycerides were quantified using a

193   colorimetric assay (ab65336, Abcam, Paris, France) of liver homogenates. All procedures

194   were authorized following review by the institutional ethic committee and carried out under

195   national licence condition (Ref 00486.02).

196   **Histology and immunohistochemistry of animal tissues**

197   Liver fibrogenesis and immunohistochemistry were determined as previously described [31].

198   An epitope-specific antibody (C27C9) was used for immunohistochemistry detection of

199   insulin on pancreas sections (8508S Ozyme, Saint Quentin en Yvelines, France).

200   **RNA isolation and quantitative RT-PCR**

201   Liver RNA preparation and reverse transcription were performed as previously reported [31].

202   Quantitative RT-PCRs were performed using oligonucleotides designed for the genes *Col1*

203   (Forward: CACCCCAGCGAAGAACTCATA; Reverse:

204   GCCACCATTGATAGTCTCTCCTAAC) and *Col3* (Forward: GCACAGCAGTCCAACGTAGA;

205   Reverse: TCTCCAAATGGGATCTCTGG) and using the cyclophilin A housekeeping

206   gene.[31]

207

208 **RESULTS**

209

210 **Hippurate is the urine metabolite most strongly associated with fecal microbial gene**

211 **richness.**

212 To identify microbial and host compounds mediating beneficial effects in metabolic health,

213 we profiled the urinary metabolome of the MetaHIT population[4] using ^{1}H nuclear magnetic

214 resonance (NMR) spectroscopy to perform a Metabolome-Wide Association Study

215 (MWAS)[11] for microbial gene richness, a proposed criterion of metabolic and immune

216 health[4] (Figure 1). We first built an orthogonal partial least squares (O-PLS) regression

217 model based on the ^{1}H NMR spectra to stratify the population by gene richness quartiles

218 computed using our previously published 10-million integrated gene catalog (IGC)[2] (Figure

219 1A, P=5.8x10^{-21}). The cross-validated model significantly predicted variance associated with

220 gene richness through a permutation test (Figure 1B, P=9.7x10^{-5}, 10,000 randomizations).

221 Model coefficients for this discrimination revealed hippurate as having the strongest

222 association with microbial gene count (Figure 1C): individuals with low microbial richness

223 present significantly lower urinary hippurate levels than individuals with high microbial

224 richness (Figure 1D, P=1.99x10^{-9}, r^2=0.173). These data support reports of association

225 between hippurate levels and microbial functional redundancy[26] and Shannon's diversity

226 index[17] (Figure1E, P=0.024 and Supplementary Figure 1A, P=0.0058).

227

228 Consistent with associations previously reported for microbial gene richness in the MetaHIT

229 population[4] and associations between hippurate and reduced cardiometabolic disease

230 risk[11,12,14,17], urinary hippurate significantly correlated with low values for body mass

231 index (BMI), bodyweight, the homeostasis model assessment of insulin resistance (HOMA-

232 IR) and fasting circulating levels of IL6, insulin, and C-peptide, whilst adjusting for age and

233 gender (partial Spearman's rank-based correlations, q<0.1, Supplementary Figure 1B).

234 Moreover, stratification on urinary hippurate concentrations in lean (BMI <25 kg/m^2), and

235 overweight or obese (BMI >25 kg/m^2) individuals showed improved glucose homeostasis in

236 participants excreting higher levels of hippurate (Supplementary Figure 1C, *median*

237 *threshold*). These observations depict hippurate, one of the main microbial-mammalian co-

238 metabolites found in human urine, as a key molecular marker associated with gene richness

239 which may underlie some of its health benefits. These results however raise questions

240 related to the entanglement of gene richness and hippurate as potential markers of

241 health[13,17]. Adjusting for hippurate weakens associations between gene richness and

242 bioclinical variables (Supplementary Figure1B), consistent with the idea that hippurate could

8

243   mediate some of the observed benefits for subjects with higher gene richness. However,

244   hippurate associations with bioclinical variables adjusted for gene richness are no longer

245   significant, suggesting that the gene richness signal overrides hippurate associations in the

246   presence of confounding variation affecting urinary concentrations, such as diet, microbial

247   synthesis, host conjugation and clearance. Hippurate did not correlate either to glycine

248   bioavailability, which is required for hippurate synthesis through conjugation with gut

249   microbial benzoate[32] or kidney function (eGFR) which could limit hippurate synthesis and

250   clearance (Supplementary Figure 1D-E).

251

252   **Microbiome determinants of hippurate production in the phenylpropanoid pathway**

253   To characterize the microbial determinants of benzoate production, we next focussed on

254   high-throughput shotgun sequencing fecal metagenomics data (n=271). We functionally

255   annotated functions of the IGC to KEGG Orthology (KO) groups and found 2,733 KEGG and

256   6,931 EggNOG modules positively associated with urine hippurate levels (pFDR<0.05,

257   Supplementary Tables S1-2). Of specifically curated enzymatic modules[26] involved in

258   microbial benzoate metabolism (4 aerobic and 15 anaerobic; Supplementary List), only three

259   modules significantly correlated with urine hippurate levels: MC0004 (detected in 271

260   samples) corresponding to a 2-enoate reductase converting cinnamic acid into 3-(3-

261   hydroxyphenyl)-propionic acid, MC0005 (observed in 201 samples) converting cinnamate

262   into benzoate and MC0014, a benzoate 4-monooxygenase only observed in fewer than 15%

263   of individuals (Figure 2A, Supplementary Table S3). Abundance of these modules also

264   correlated with gene richness (Supplementary Table S4), thereby providing a functional

265   basis for the association between gene richness and urine hippurate levels observed in this

266   population (Figure 1). Genes involved in MC0004 and MC0005 were predominantly found in

267   genomes from unclassified Firmicutes and Clostridiales (Figure 2B, Supplementary Tables

268   S5-6). Among classified Firmicutes, the genera *Lachnoclostridium*, *Eubacterium* and *Blautia*

269   harbored MC0004. Conversely, MC0005 was encoded by Proteobacteria, i.e. *Klebsiella*,

270   *Enterobacter*, *Suterella* and *Comamonas* (Figure 2B). We then mapped these modules into

271   the enteroscape (as observed on the principal coordinates plot derived from normalized

272   genus abundances using Bray-Curtis distances,[26] Figure 2C), revealing that the

273   conversion of cinnamic acid into 3-hydroxy-3-phenylpropionic acid is linked to the

274   *Ruminococcus* enterotype, while capacity to convert cinnamate to benzoate is more

275   ubiquitously distributed across gut community types. Phenylpropanoid pathway potential is

276   increased in the *Ruminococcaceae*-enterotype compared to the *Bacteroides*- or *Prevotella*-

277   enterotypes, the former being confirmed by analyzing gradients of key taxa instead of

9

278   enterotypes (Supplementary Table S7). The results altogether suggest a wide range of

279   substrates, taxa and species are involved in benzoate production, consistent with its

280   association with gene richness.

281

282   **Urine hippurate levels associate with improved metabolic health in patients with diets**

283   **rich in meat and saturated fats**

284   We next assessed individual nutritional intake through validated FFQs available in 193

285   MetaHIT individuals.[19] Associations with metabolic health were stratified according to

286   multivariate dietary patterns (Figure 3). A PCA of 133 dietary intake descriptors summarises

287   dietary patterns and loadings highlight four archetypal diets within our population: higher

288   consumption of fruits and vegetables (n=96) vs. high consumption of meat containing

289   saturated fats (n=97) on the first principal component (PC1) and carbohydrate-rich foods vs.

290   fish containing unsaturated fats on PC2 (Figure 3A), a trend which was observed at the food

291   ingredient and nutrient level (Supplementary Figure 2A-B). It is therefore possible to stratify

292   the population according to the median of dietary PC1 highlighting contrasts between

293   healthy (higher consumption of fruit and vegetables) and at-risk (higher consumption of

294   carbohydrates and meat) diets. Although hippurate was not correlated with the first two

295   dietary principal components, its dynamic range was similar whilst stratifiying according to

296   the first two principal components (Supplementary Figure 2C-E). To summarise the main

297   factors influencing inter-individual variation in urine hippurate excretion, we calculated the

298   cumulative contribution of several covariates using a dbRDA ordination approach (Figure

299   3B). Gene richness accounted for 12% (P=0.002), followed by MC0020 encoding a

300   hippurate dehydrolase (4%, P=0.002, observed in 271 subjects) catalysing the

301   retroconversion of hippurate into benzoate, and HOMA-IR (1.5%, P=0.008; n=265). When

302   taking diet into account (i.e., PC1 fruits and vegetables vs. meat; n=193) in the dbRDA, gene

303   richness contributes to 15% (P=0.002), diet adding another 4% (P=0.002) and hippurate

304   retroconversion 3% (P=0.004), suggesting that the pattern of hippurate associations could

305   be diet-dependent and requiring further analysis. We therefore stratified the data according

306   to diet (n=193) using a median threshold for the first dietary principal component,

307   highlighting a healthy diet associated with vegetables and fruit intake (low PC1 values, n=96)

308   and an at-risk diet rich in saturated fats derived from meat intake (n=97). For this latter

309   subset of individuals consuming a diet rich in saturated fats on the first dietary principal

310   component, urine hippurate levels significantly associated with decreased HOMA-IR,

311   circulating fasting levels of insulin, fasting associated adipocyte factor (FIAF, also known as

312   Angiopoietin-like 4, a peroxisome proliferator-activated receptor target gene environmentally

10

313   modulated by the gut microbiota inhibiting lipoprotein lipase in adipose tissue [33]) and TNF-

314   α, whilst displaying increased plasma levels of fasting adiponectin (Figure 3C-E,

315   Supplementary Table S8). Urine hippurate was not associated with any health benefits in the

316   subsets of participants consuming mostly a fruit and vegetable diet, a pescetarian diet or a

317   carbohydrate-rich diet (Supplementary Table S8).

318

319   To disentangle contributions arising from hippurate and gene richness to bioclinical variables

320   in subjects consuming a diet rich in fats, we compared unadjusted and adjusted Spearman's

321   rank-based correlations (Figure 3H). In the population consuming higher amounts of meat

322   and saturated fats, elevated urine hippurate levels significantly associated with an increase

323   in fasting plasma adiponectin and a reduction in adiposity, BMI, HOMA-IR and fasting

324   plasma insulin, which is consistent with gene richness being significantly associated with an

325   increase in adiponectin and a decrease in HOMA-IR and fasting plasma insulin. However,

326   the associations between gene richness and bioclinical variables were no longer significant

327   when adjusting for urine hippurate levels. Conversely, hippurate associations with insulin

328   and HOMA-IR were still significant after gene richness adjustment. We exemplified this

329   through a correlation graph taking into account the correlation between hippurate and gene

330   richness (r=0.44): this unadjusted correlation between gene richness and HOMA-IR

331   collapses when adjusting for gene richness (rho=0.143, n.s.) and is in fact contributed for by

332   a partial correlation between urine hippurate and HOMA-IR (Figure 3I). The latter finding

333   suggests a possible preventive role for hippurate in metabolic disease driven by diets high in

334   meat and saturated fats, independently of gene richness.

335

Hippurate and benzoate improve glucose tolerance in HFD-fed mice

337   To further study the impact of benzoate and hippurate on host physiology, we treated mice

338   with subcutaneous infusion of hippurate (0.14 mg/kg/day) and benzoate (0.1 mg/kg/day) in

339   CHD and HFD (Figure 4). Under control diet, metabolite treatments had no effect on body

340   weight, BMI and fasting glycemia (Supplementary Figure 4). Benzoate caused a significant

341   elevation of the adiposity index and a reduction of the normalised heart weight

342   (Supplementary Figure 5A). During an IPGTT, both metabolites induced a slight increase in

343   glycemia (Figure 4A-B) and ΔG parameter (Figure 4C), respectively. Also, hippurate induced

344   a stronger glucose-stimulated insulin secretion than benzoate, compared to the saline-

345   treated mice (Figure 4D). Whilst HFD-feeding increased body weight and adiposity,

346   hyperglycemia and glucose intolerance (Figure 4E-H, Supplementary Figs 4D,E and 5),

347   mice treated with hippurate or benzoate showed a parallel improvement in glucose tolerance

11

348   compared to saline-treated controls (Figure 4E). This effect was illustrated by the highly

349   significant reduction of both the cumulative glycemia during the test (Hippurate vs. control -

350   23.90% P=0,001, benzoate vs. ctl -31.52%, P=0.001) and the ΔG parameter (Hippurate vs.

351   ctrl -37.22% P=0,001, benzoate vs ctrl -33.35%, P=0.001) (Figure 4F,G). Hippurate and

352   benzoate treatments also significantly increased glucose-induced insulin secretion (Figure

353   4H). These data suggest that both metabolites have the capacity to improve glucose

354   tolerance and stimulate glucose-induced insulin secretion *in vivo* specifically in diet-induced

355   obesity and diabetes.

356

357   **Effects of hippurate and benzoate on the morphology of pancreatic islets**

358   To investigate the possible cause of stimulated insulin secretion by hippurate and benzoate,

359   we performed out a histological analysis of pancreatic islet structure. We confirmed that

360   insulin positive area was increased by hippurate (+194%, P=0.04, one-tailed) or benzoate

361   (+437%, p=0.02, one-tailed) respectively in mice fed control diet (Figure 5); hippurate

362   treatment Insulin positive area was also increased in HFD-fed mice treated with hippurate

363   (+168%, P=0.04, one-tailed). These data suggest that increased β-cell mass may explain

364   enhanced insulin production and secretion induced by hippurate and benzoate treatment.

365

366   **Effects of hippurate and benzoate on liver histopathology and function**

367   Liver triglyceride accumulation, fibrosis and inflammation are hallmarks of structural and

368   biochemical adaptations to HFD feeding. Liver triglycerides were more elevated in HFD fed

369   mice (29.30±4.15 mg/g) than in mice fed control diet (8.63±2.19 mg/g, P=0.002)

370   (Supplementary Figure 6). Hepatic triglycerides were not significantly affected by hippurate

371   or benzoate treatment in either diets. Benzoate induced a singifnicant decrease in liver

372   triglycerides compared to hippurate in HFD (-57.35%, P= 0.02) (Supplementary Figure 6).

373   We next analysed hepatic fibrosis through quantitative analysis of collagen detected by red

374   picrosirius staining of histological sections (Figure 6A). Hippurate treatment resulted in a

375   marked reduction of liver collagen in mice fed control diet (-53.2%) or HFD (-55.7%),

376   whereas benzoate had no effects on collagen levels in these mice (Figure 6B,C). These

377   results were confirmed by liver expression of the genes encoding collagen 1 (*Col1*) and

378   collagen 3 (*Col3*) (Figure 6B,C): hippurate treatment induced a significant reduction of the

379   expression of *Col1* (-79.89%, P=0.02) and *Col3* (-29.37%, P=0.01) under control diet (Figure

380   6B). but the effect of the metaolites on *Col1* and *Col3* I HFD was marginal (Figure 6C).

381   Finally, we assessed the effects of hippurate and benzoate on liver inflammation through α-

382   SMA (alpha Smooth Muscle Actin) staining[34,35] (Figure 7A), which is increased by HFD-

12

383   feeding (+273.86%) (Figure 7B,C). Hippurate induced a marked reduction in α-SMA staining

384   in mice fed control diet (-82.71%) or HFD (-94.87%) (Figure 7B,C), suggesting reduced

385   presence of stellar cells and reduced liver inflammation when compared to saline-treated

386   controls. In contrast, benzoate treatment in chow diet induced a strongly significant increase

387   in stellar cells when compared to mice treated with saline (+564%, P=10^{-7}) or hippurate

388   (+3,741%, P=10^{-7}), thereby indicating liver inflammation in these mice (Figure 7B).

389   Collectively, these data show that hippurate decreases fibrosis and inflammation regardless

390   of diet, whereas benzoate reduces triglycerides and collagen accumulation in obese mice

391   fed HFD whilst stimulating inflammation in lean mice fed control diet.

392

393   **DISCUSSION**

394

395   Integrated analysis of metabolome profiling and deep metagenome sequencing data of 271

396   middle-aged non-diabetic Danish subjects from the MetaHIT study sample [4] identified

397   urinary hippurate as the metabolite most significantly associated with microbial gene

398   richness based on the microbial IGC.[2] This observation largely confirms previous reports

399   associating hippurate with gene richness in steatosis and bariatric surgery contexts[14,36]

400   as well as with increased gut microbial diversity as assessed by sequencing the 16S rRNA

401   gene amplicon.[17] Hippurate having previously been inversely correated with blood

402   pressure, obesity and steatosis,[11-14] this study highlights diet-dependent relationships

403   between microbiota-host co-metabolism of benzoate and hippurate and health benefits

404   associated with gene richness. Our in-depth dissection of the metagenomic determinants of

405   urinary hippurate highlighted a series of richness-responsive gene modules functionally

406   related to benzoate synthesis. These modules are shared across several enterotypes and

407   taxonomic gradients. Population stratification analyses demonstrated that hippurate only

408   benefits individuals consuming a diet rich in saturated fats. This hypothesis of a diet-

409   dependent beneficial health effect of benzoate metabolism was confirmed *in vivo* in a

410   preclinical model of HFD-induced obesity.

411

412   **Hippurate brings diet-dependent metabolic improvements in pancreas and liver**

413   Our study shows that chronic hippurate treatment in a model of obesity induced by HFD-

414   feeding reduces glucose intolerance, stimulates insulin secretion, enhances β-cell mass and

415   reduces hepatic inflammation and fibrosis. Metabolomic studies have consistently shown

416   inverse associations variations between hippurate levels and pathophysiological elements of

417   the metabolic syndrome. Urinary hippurate is reduced in mouse models of insulin

13

418 resistance[10] and in rat models of spontaneously occurring hypertension (SHR), type 2

419 diabetes (Goto Kakizaki, GK) and obesity (Zucker) or the WKY rat.[37-39] This is consistent

420 with our previous reports showing an inverse association among hippurate, insulin

421 resistance, hypertension, obesity or liver steatosis[10-12,14] and observations that hippurate

422 exerts protective effects in β-cells.[40] We also showed in HFD-fed isogenic mice that

423 urinary hippurate measured before a 3-week HFD induction predicts the future development

424 of obesity, suggesting that functional variations in microbiome predicts disease risk

425 independently of genetics.[41] Whilst both hippurate and benzoate have similar *in vivo*

426 effects, including greatly improved glucose tolerance and stimulation of insulin secretion,

427 only hippurate results in beneficial effects on increased β-cell mass or reduced liver fibrosis.

428

429 **The phenylpropanoid-benzoate-hippurate pathway in metabolic health**

430 The range of responses observed in the animal model treated with hippurate and benzoate

431 depict subtle and context-dependent microbiome–host interactions. Benzoate and its co-

432 metabolite hippurate are the endproducts of several converging microbial biosynthetic

433 pathways.[15] The phenylpropanoid pathway is a broad network of reactions connecting a

434 wide range of dietary substrates such as phenylalanine, quinic acid, shikimic acid or

435 chlorogenic acid for instance to 4-coumaryl-coA. These pathways lead to much simpler

436 molecules, benzoate being their common endpoint. Dietary and microbial intermediates

437 (including cinnamic acids, coumarins, stillbenoids, flavonoids and isoflavonoids) in the

438 phenylpropanoid and connected pathways are associated with beneficial health

439 outcomes.[15,42]

440

441 **Conclusion.** Our study depicts hippurate as a pivotal microbial-host co-metabolite mediating

442 part of the beneficial metabolic improvements associated with high microbial gene richness

443 in the context of Western-style diets. This work unifies previous reports in which hippurate

444 was associated improvements in insulin resistance, steatosis, hypertension and obesity[10-

445 12,14] and microbial ecological diversity.[14,17] Beyond the diversity of microbial

446 ecosystems and functions associated with hippurate, we uncover beneficial bioactivities in

447 the liver and pancreas resulting in health benefits in terms of metabolic control, liver

448 inflammation and fibrosis. Our observations support the existence of diet-dependent

449 microbial-host metabolic axis in which hippurate partly offsets unhealthy diets, further

450 exemplifying that the microbiome determines key components of human biochemical

451 individuality[43] and provides critical diagnostic and therapeutic potential in personalized

452 nutrition and stratified medicine.[44,45]

14

463 **Contributions**

464 F.B. J.C., T.N. and S.V.S. and contributed equally to this work. F.B. J.C. and G.I.M. acquired

465 data, J.C., T.N., S.V.S. performed analyses, G.F. and S.V.S. curated the gut-specific

466 metabolic modules, L.H., A.L.N., A.R.M., N.P., S.F., E.L.C., and A.M.L.L. participated in data

467 collection and processing, J.C., T.N., S.V.S., F.B and G.F. performed statistical analyses.

468 M.-E.D., D.G., J.R. and O.P. designed the study. T.H., J.K.N. K.C., P.B., S.D.E., participated

469 in the study design and interpretation of the results, M.E.D. wrote the manuscript with

470 contributions from F.B., J.C., T.N., S.V.S, G.F., J.R., O.P and D.G.

471

472 **Competing interests**

473 The authors declare no competing financial interests.

15

474 **Figure Legends**
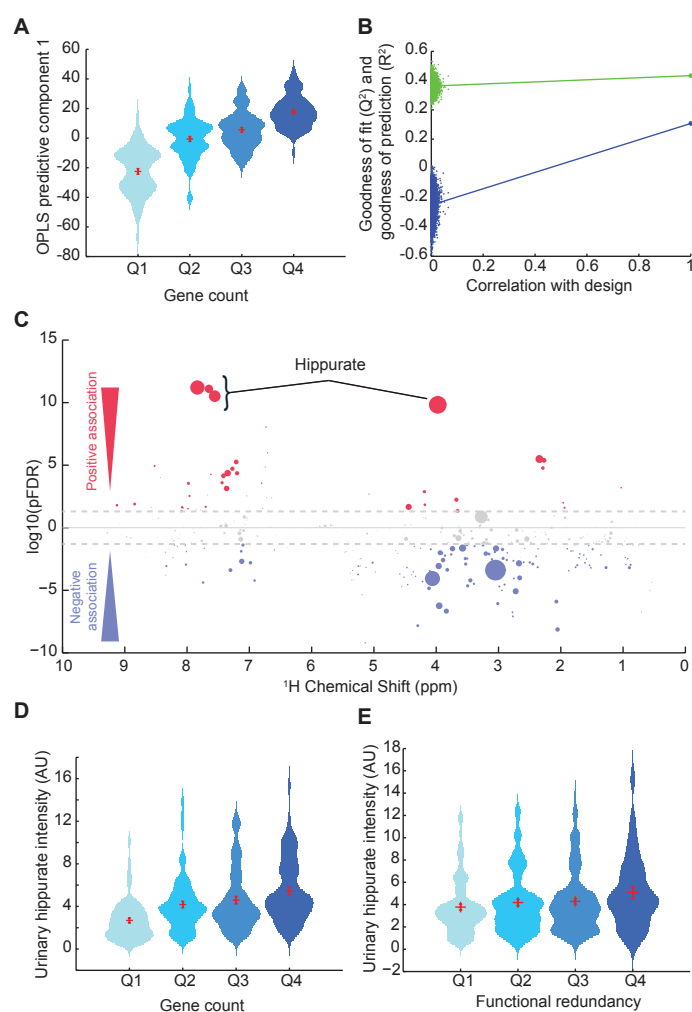
475

476 **Figure 1. Hippurate is the main metabolite correlated with gene richness and**

477 **functional redundancy of the microbiome. (A)** Scores plot (predictive component 1)

478 obtained for an O-PLS-DA model fitted usingurinary^{1}H NMR-spectra to predict microbial

479 gene richness, showing a significant association between gene richness quartiles and ^{1}H

480 NMR spectra (p=5.84x10^{-21} for a significantly non-zero slope using F-test, n=271). **(B)**

481 Empirical assessment of the significance of O-PLS goodness-of-fit parameter Q^2_{Yhat} by

482 generating a null distribution with 10,000 random permutations (p=9.68x10^{-5}). **(C)** Manhattan

483 plot highlighting associations between ^{1}H NMR variables and gene count displayed in a

484 pseudo-spectrum layout. A negative value (blue circles) means a negative correlation while

485 a positive value (red circles) means a positive correlation. Grey circles are clusters with a p-

486 value>0.01. Size of circles represents the covariance of the cluster with the gene count.**(D)**

487 Association between urinary hippurate intensity and gene count quartiles (p=1.99x10^{-9} for a

488 significantly non-zero slope using F-test). **(E)** Association between urinary hippurate intensity

489 and microbial functional redundancy [26] quartiles (p=0.0239 for a significantly non-zero

490 slope using F-test, n=271).

16
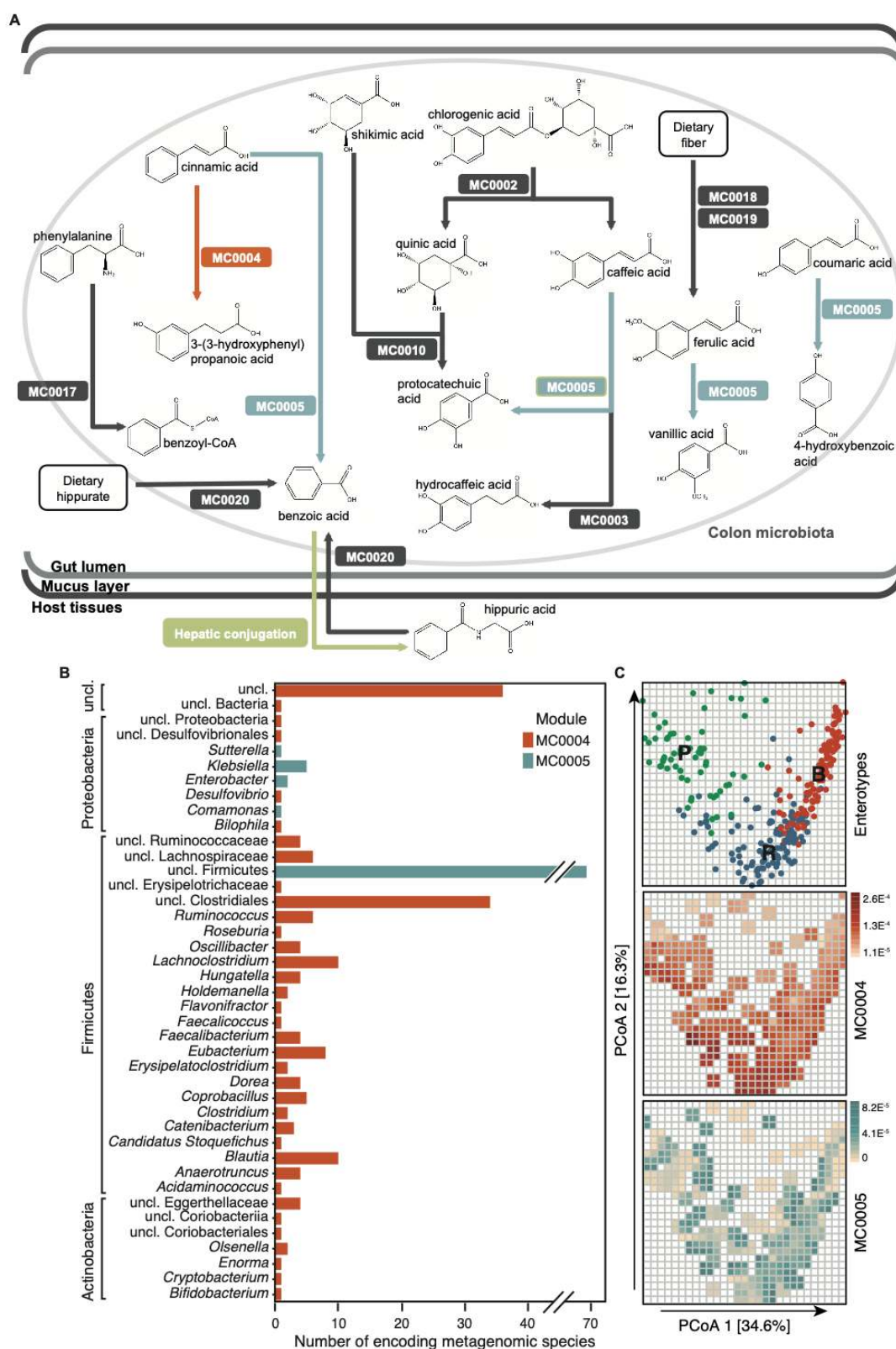
Figure 2. Detection of microbial phenylpropanoid metabolism-related modules in fecal metagenomes of healthy volunteers and their associations with urine hippurate concentrations. (A) Visualisation of gut-specific metabolic modules (GMMs) encoding anaerobic phenylpropanoid metabolism-related pathways detected in more than 20% of

17

496   individuals; MC0004 (orange; Spearman rho=0.19, q-value=0.005) and MC0005 (blue;

497   Spearman rho=0.21, q-value=0.005) correlate positively to urine hippurate concentrations

498   (n=271). All metabolites are connected to benzoate but for clarity the non-significant

499   reactions were omitted. **(B)** Metagenomic species encoding modules MC0004 and MC0005.

500   **(C)** [top panel] Fecal microbiomes dissimilarity visualised on the first plane of the genus-level

501   principal coordinates analysis (PCoA, Bray-Curtis dissimilarity), with individual samples

502   colored according to enterotypes (R, Ruminococcaceae; B, Bacteroides; P, Prevotella).

503   [middle and bottom panels] Same genus-level PCoA overlaid with a mesh colored according

504   to the median abundances of GMMs MC0004 (red) and MC0005 (blue) in samples falling

505   within each cell of the mesh (n=271). See Supplementary Table S3 for correlation between

506   hippurate and GMMs.

18
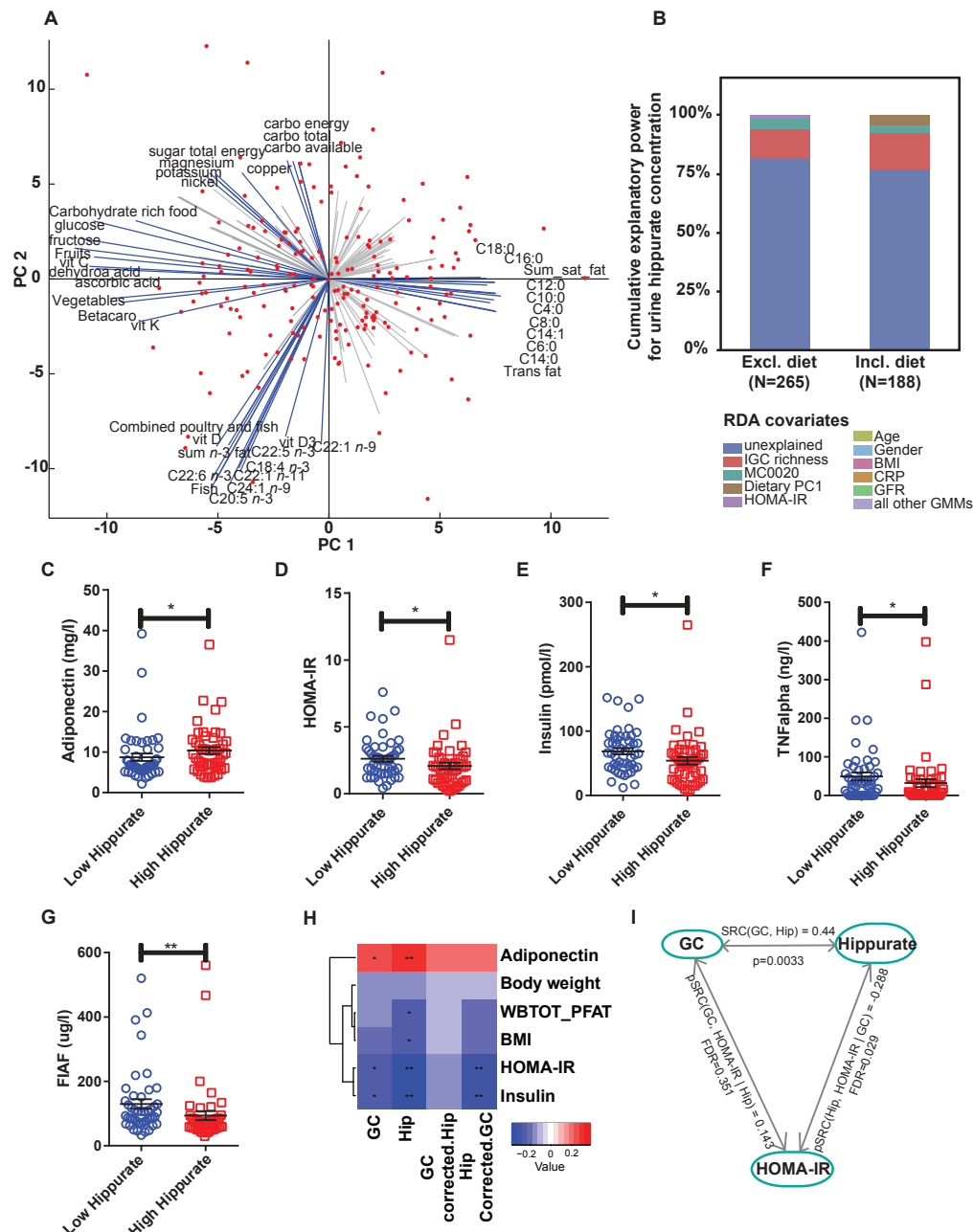
507

Figure 3. Hippurate associates with improved glucose homeostasis only in participants consuming a diet rich in saturated fats. (A) Biplot of the principal component analysis (PCA) of dietary intakes highlights opposite diets along first two principal components (PCs). The main drivers of each principal components are named and represented by blue arrows. **(B)** Cumulative contributions of explanatory variables to inter-individual variation in hippurate excretion, estimated by redundancy analysis (dbRDA). Explanatory variables included microbiota gene count, microbiota phenylpropanoid metabolism modules, host dietary principal components and clinical parameters (age, gender, BMI, HOMA-IR, CRP, serum glycine levels, and glomerular filtration rate (eGFR) estimation with CKD-EPI). **(C-F)** Evaluation of hippurate stratification (high hippurate, n=49

19

518   vs low hippurate, n=48) on bioclinical variables (q<0.1, Supplementary Table S8) for

519   individuals on high PC1 (i.e. high meat / high saturated fat diet). For full name description of

520   physiological data see Supplementary Table S8.

521

522
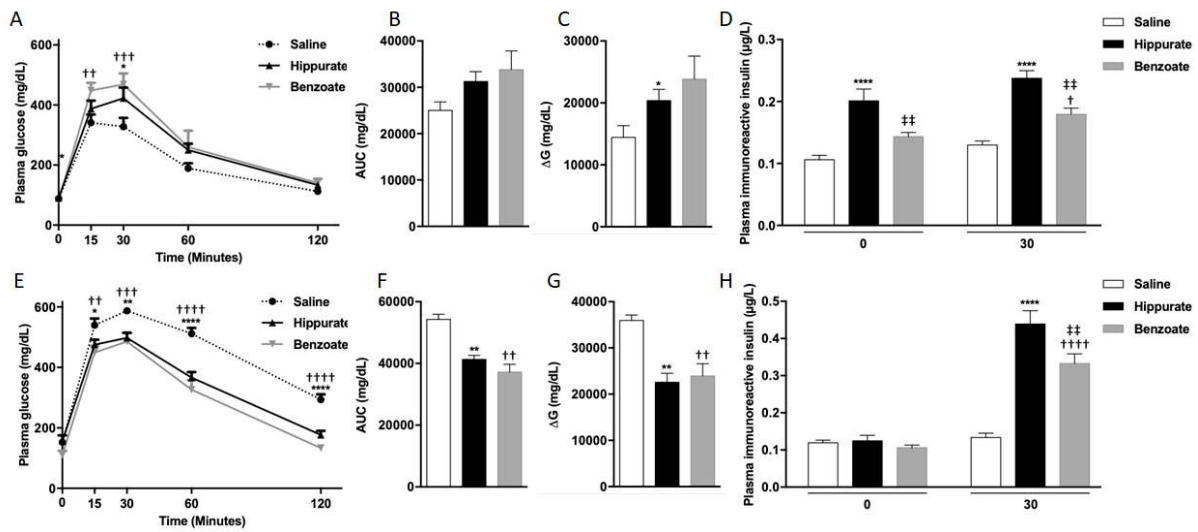
523

524 **Figure 4. Chronic hippurate treatment improves glucose homeostasis in HFD-fed**

525 **mice.**

526 **(A)** Heatmap summarising Spearman's partial correlation between gene richness,

527 hippurate,gene richness adjusted for hippurateand hippurate adjusted for gene richness and

528 bioclinical variables, all correlations adjusted for age and gender. Stars represent significant

529 pFDR corrected using Benjamini Hochberg procedure * pFDR<0.1, ** pFDR<0.05, ***

530 p<0.01. **(B)** Representation of the Spearman's correlations and partial correlations between

531 gene count and hippurate, hippurate and HOMA-IR adjusted for gene richness and between

532 gene richness and HOMA-IR adjusted for hippurate. **(C)** Plasma glucose during a glucose

533 tolerance test (GTT). **(D)** Area under the curve for glucose during the GTT. **(E)** Body weight

534 of mice during the 6 weeks of hippurate treatment. **(F)** Body mass index at sacrifice **(G)**

535 Adipose tissue weight normalised to body weight. **(H)** Plasma adiponectin concentration. For

536 chow diet and chow diet + hippurate, (n=10) and for HFD and HFD + hippurate (n=6). Data

537 shown are mean±SEM. Statistical analysis was performed using two-way ANOVA with

538 Tukey's posthoc test. ** p<0.01, **** p<0.0001. For panel (D), (F), (G) and (H), groups with

539 different superscript letters are significantly different (P<0.05), according to Tukey's posthoc
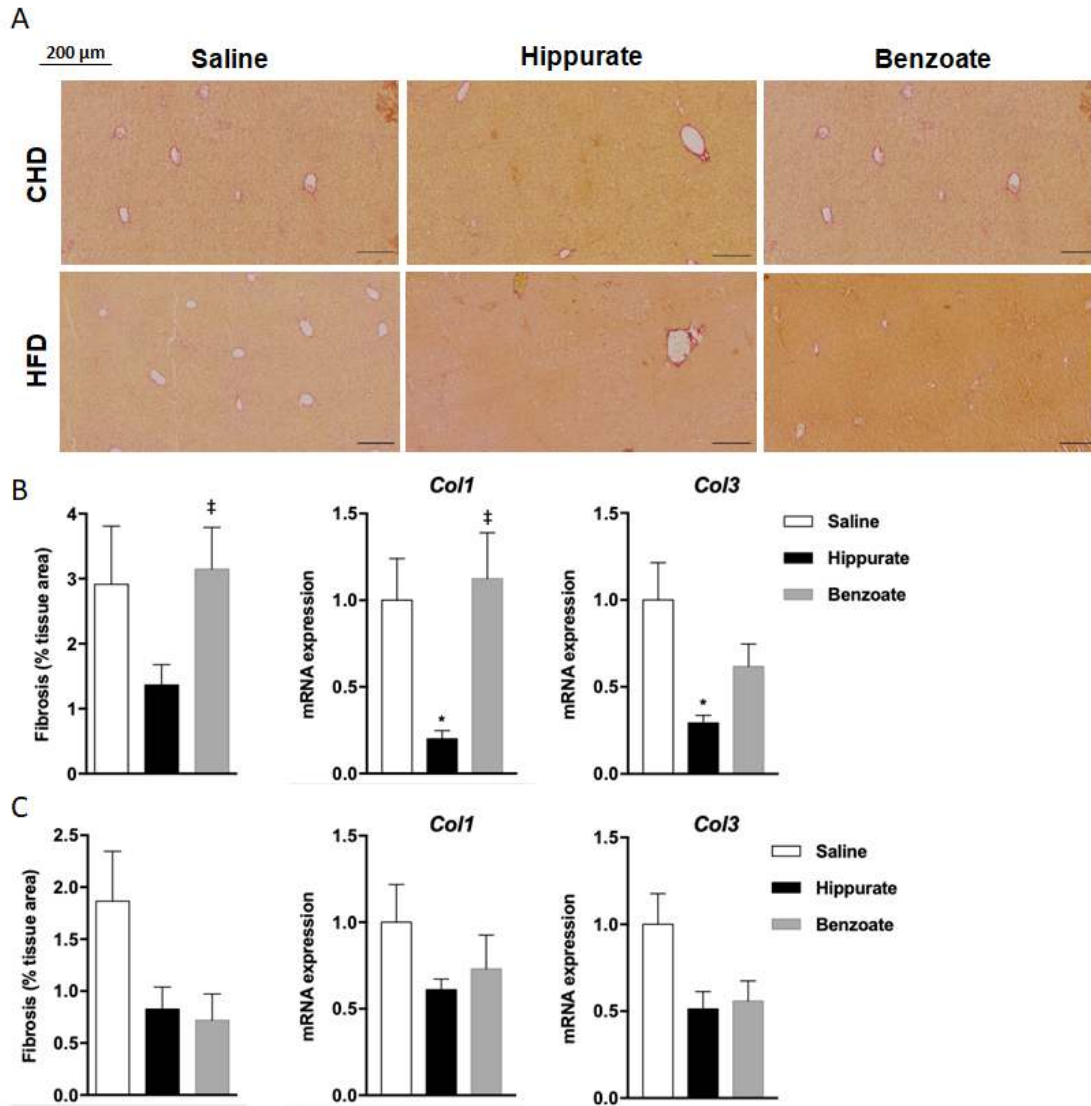
540 test.

541

542

21
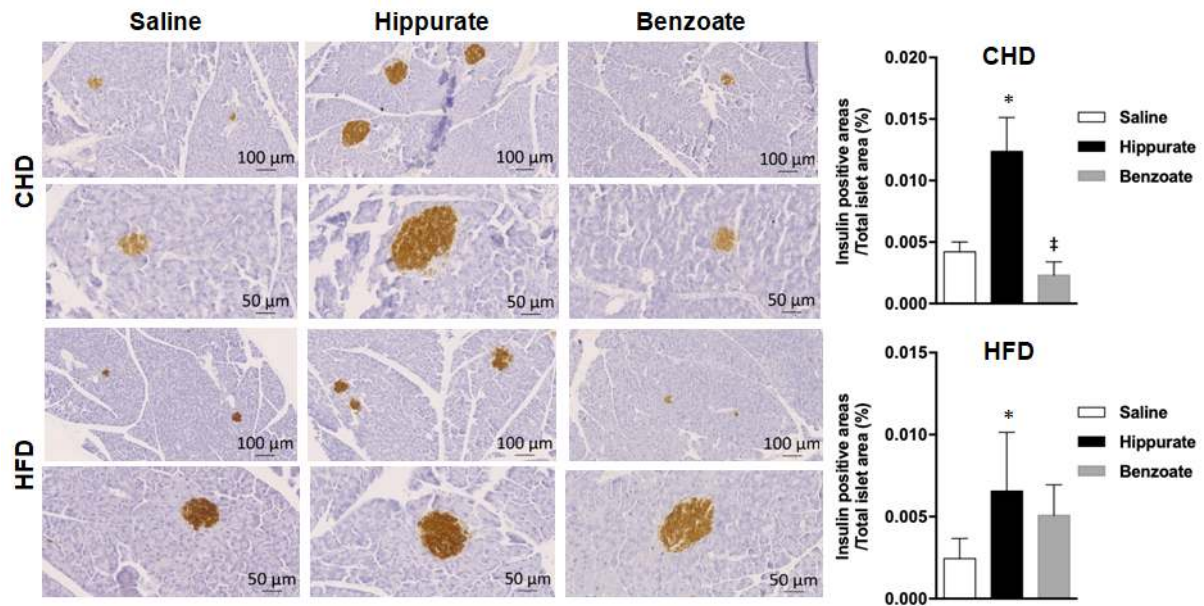
Figure 5. Effect of chronic administration of hippurate and benzoate on pancreatic islets in C57BL6/J mice. The effect of chronic subcutaneous administration of the metabolites (5.55 mM) for 42 days on islet density was tested in mice fed chow diet (CHD) or high fat diet (HFD) for 56 days. Control mice were treated with saline. Each biological replicate represents one slide per animal mounted with at least 3 tissue sections, representing 3 technical replicates, the mean and variance of which is presented as the result per biological replicate. Results are expressed as percentage of positive pixels. ‡$P < 0.05$, significantly different between mice treated with benzoate and hippurate.

Figure 6. Effect of chronic administration of hippurate and benzoate on liver fibrosis in C57BL6/J mice. (A)The effect of chronic subcutaneous administration of the metabolites (5.55 mM) for 42 days on liver collagen was tested in mice fed control chow diet (CHD) or high fat diet (HFD) for 56 days. Control mice were treated with saline. Red Picrosirius staining of histological sections was used to visualise and quantify fibrosis in mice fed CHD **(B)** or HFD **(C)**. Each biological replicate represents one slide per animal mounted with at least 3 tissue sections, representing 3 technical replicates, the mean and variance of which is presented as the result per biological replicate **(B,C)**. Liver expression of the genes enc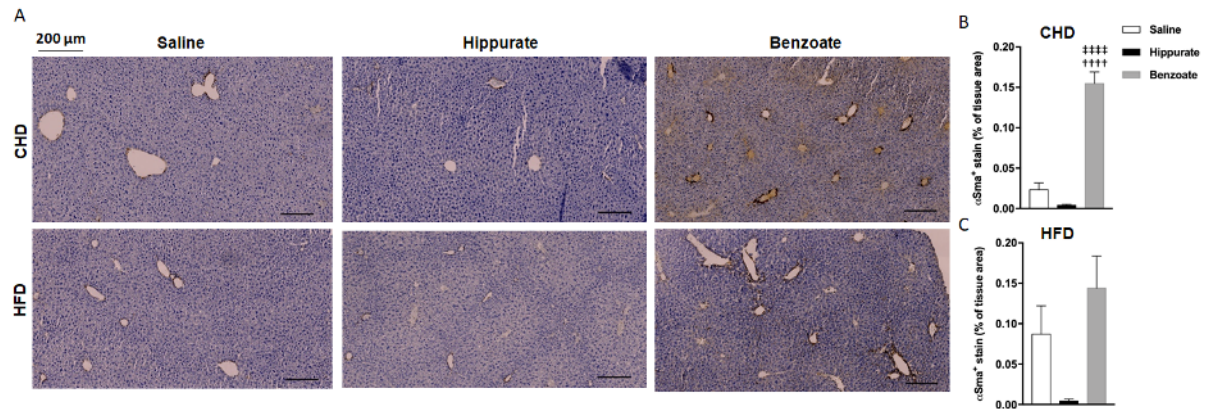oding collagen 1 (*Col1*) and collagen 3 (*Col3*) was assessed in mice fed CHD (B) or HFD **(C)** by quantitative RT PCR in 6 mice per group. Data were analyzed using the unpaired Mann-Whitney test. Results are means ± SEM. *P<0.05 significantly different between mice treated with hippurate and controls. ‡P<0.05, significantly different between mice treated with benzoate and hippurate.

Figure 7. Effect of chronic administration of hippurate and benzoate on liver inflammation in C57BL6/J mice. αSMA staining of liver slides was used to assess inflammation in mice fed chow diet (CHD) or high fat diet (HFD) for 56 days and chronically treated with subcutaneous administration of the metabolites (5.55mM) for 42 days **(A)**. Control mice were treated with saline. Each biological replicate represents one slide per animal mounted with at least 3 tissue sections, representing 3 technical replicates, the mean and variance of which is presented as the result per biological replicate in mice fed CHD **(B)** or HFD **(C)**. Data were analyzed using the unpaired Mann-Whitney test. Results are means ± SEM.

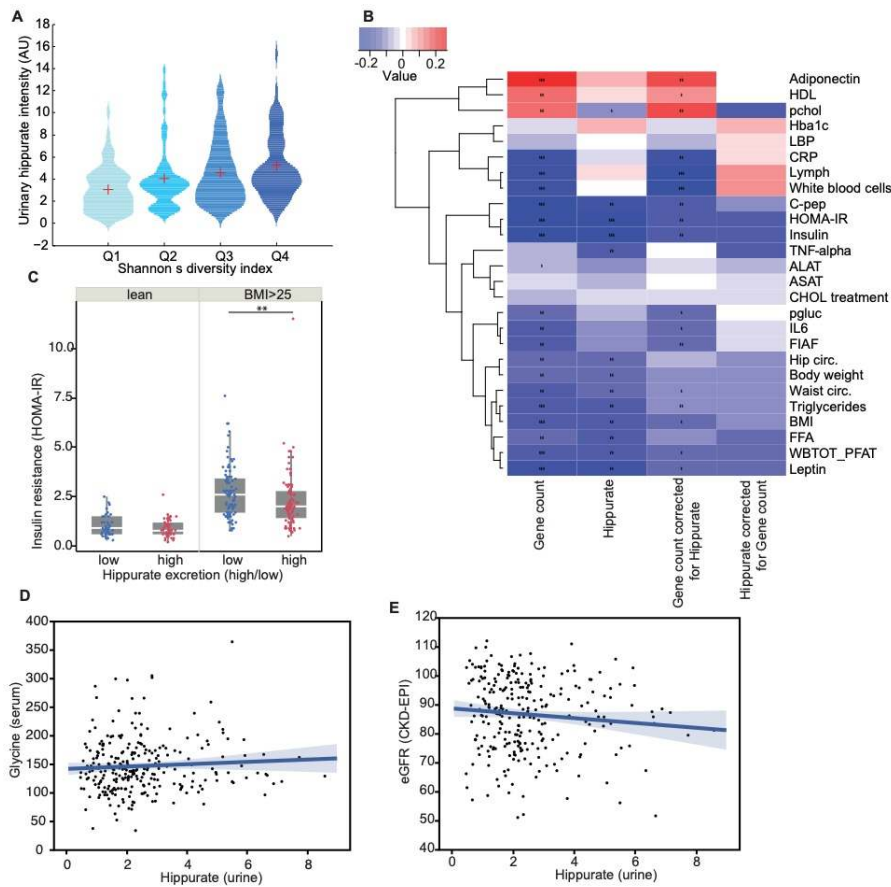††††P<0.0001, significantly different between mice treated with benzoate and saline treated controls. ‡‡‡‡P<0.0001, significantly different between mice treated with benzoate and hippurate.

580   **SUPPLEMENTARY SECTION**

581

582

583   **Supplementary Figure 1. Relationship between gene richness, hippurate and**

584   **bioclinical variables**

585   **(A)** Association between urinary hippurate intensity and Shannon's diversity index quartiles

586   (p=6.04x10^{-8} for a significantly non-zero slope using F-test, n=271). **(B)** Heatmap

587   summarising significant (pFDR<0.1) Spearman's correlation FDR corrected using Storey's

588   procedure[27] betweengene count, hippurate and gene count adjusted for hippurate and

589   physiological data, all adjusted for age and gender.For full physiological data names and

590   units see *Supplementary Table 8*. **(C)** Association between hippurate and insulin resistance

591   (HOMA-IR) stratified according to BMI (lean (BMI≤25, n=87), overweight and obese (BMI>25

592   ,n=184) and hippurate excretion levels (Mann-Whitney U test, p=0.0058). **(D)**

593   Representation of the absence of significant correlation between urinary hippurate and

594   eGFR. **(E)** Representation of the absence of significant correlation between urinary

595   hippurate and circulating glycine.

596
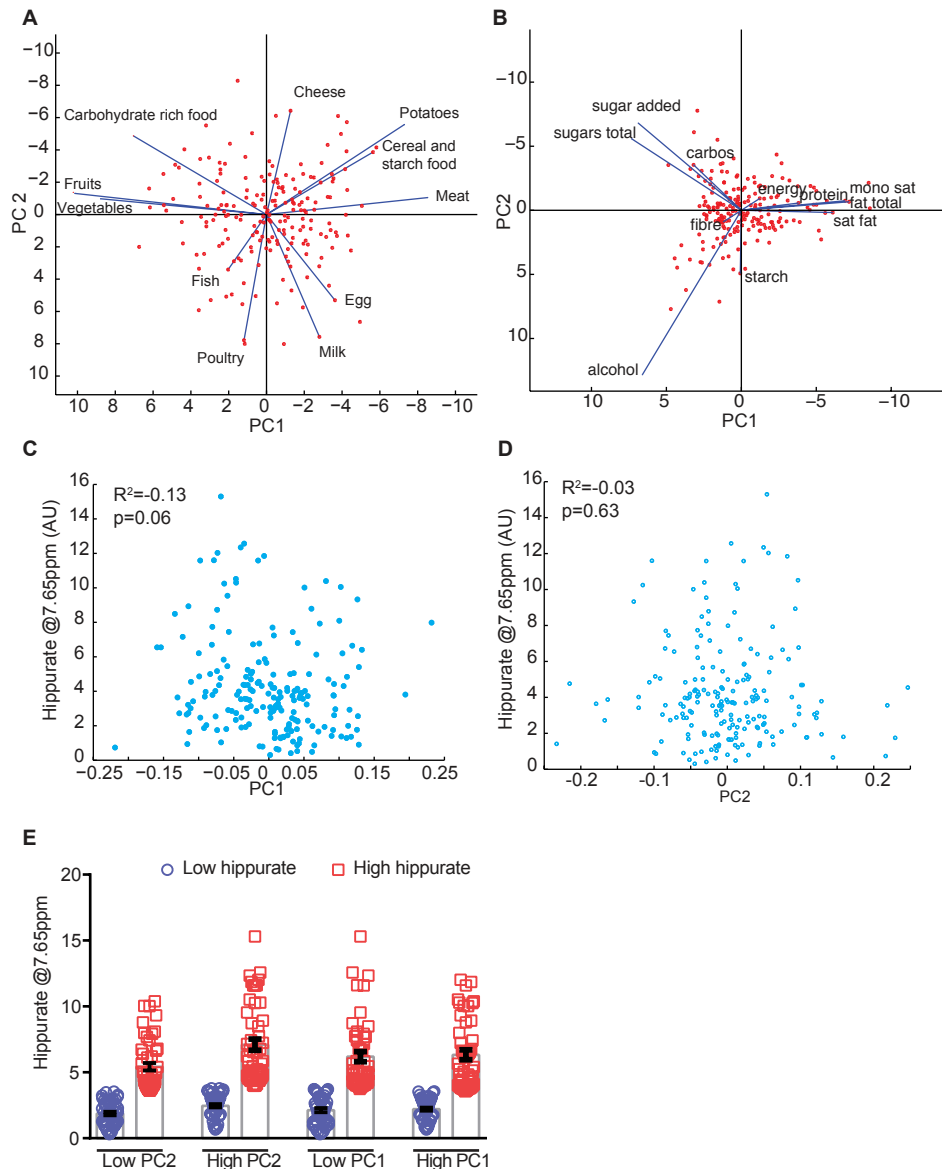
Supplementary Figure 2. Urinary hippurate does not correlate with main dietary trends summarized and presents a high variability within each subgroup

(A) Biplot of the dietary data generated using only food items. **(B)** Biplot of thmicrobial e dietary data generated using only macronutrients items. **(C)** Representation of the absence of correlation between hippurate concentration and principal component 1. **(D)** Representation of the absence of correlation between hippurate concentration and principal component 2. **(E)** Distribution of hippurate urinary concentration within each individualsubgroup stratified in high and low hippurate using median.

605
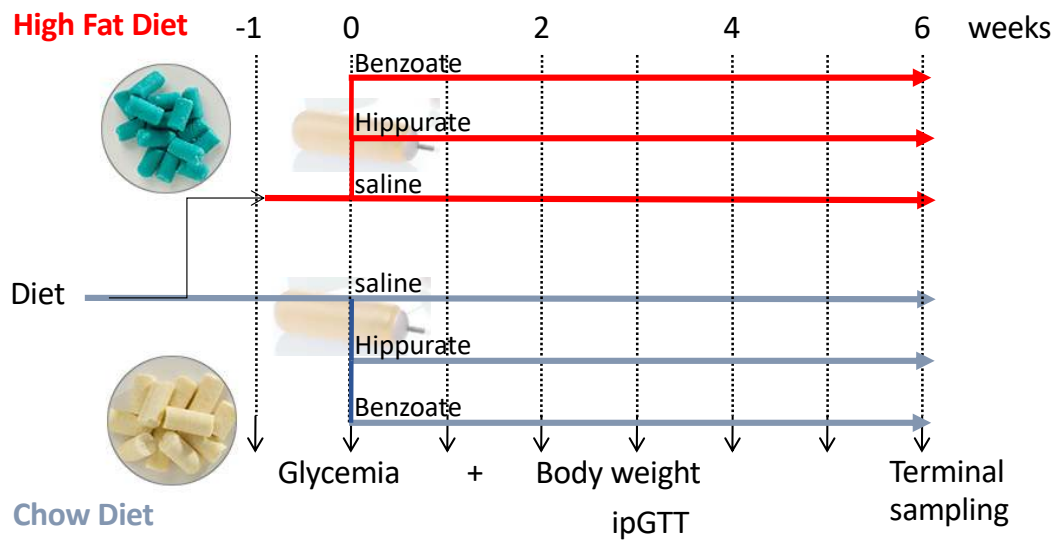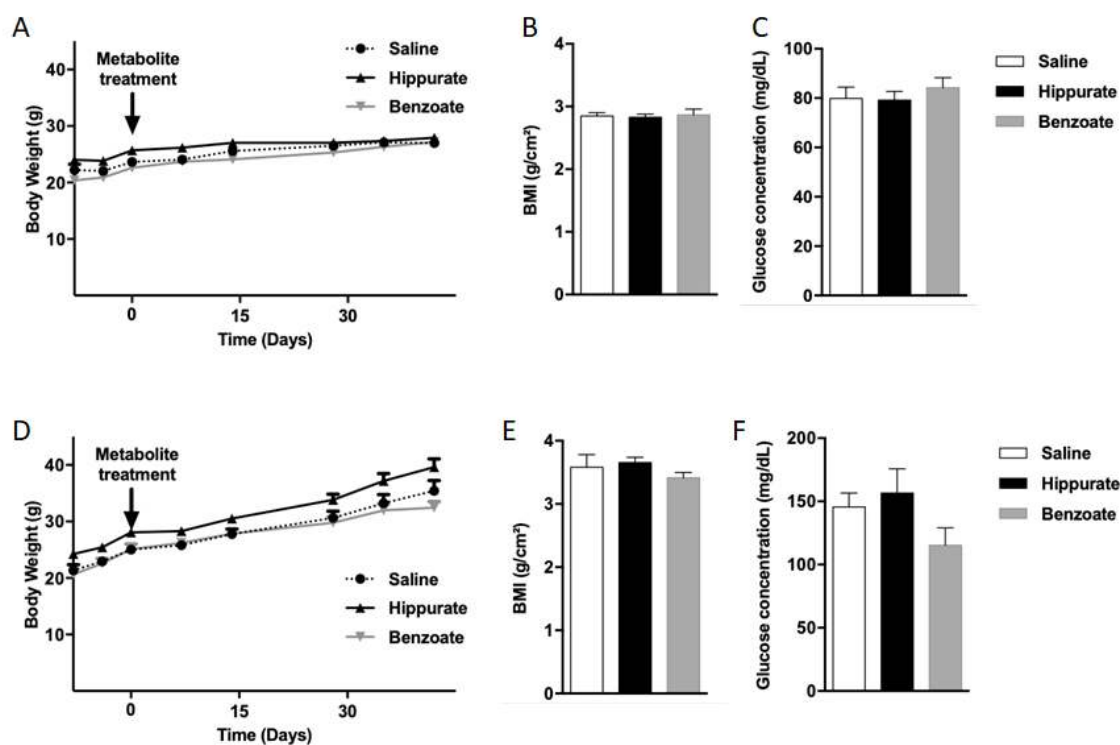
Supplementary Figure 3. Experimental design for chronic six-week administration of benzoate and hippurate

Experiment design showing groups and durations of each step for the chronic treatments with benzoate and hippurate in mice.

610

611

612

Supplementary Figure 4. Effects of chronic administration of hippurate and benzoate on body growth and fasting glycemia. C57BL6/J mice fed control chow diet **(A-C)** or high fat diet **(D-F)**. The effects of chronic subcutaneous administration of the metabolites (5.55 mM) in mice were tested on body weight **(A,D)**, body mass index (BMI) **(B,E)**, fasting glycemia **(C,F)**. Control mice were treated with saline. BMI was calculated as body weight divided by the squared of anal-nasal length. Results are means ± SEM.
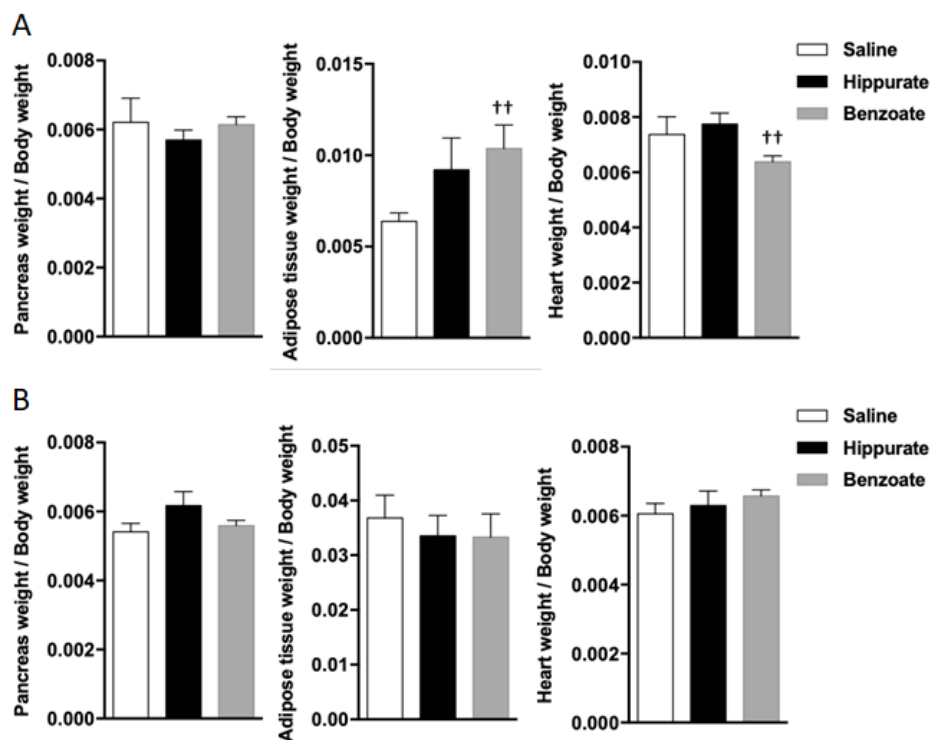
Supplementary Figure 5. Organ weight in C57BL6/J mice treated chronically with hippurate or benzoate for 42 days. Control mice were treated with saline. Mice were fed chow diet (CHD) or high fat diet (HFD) for 56 days. Data are expressed as the ratio between organ weight and body weight. Data were analyzed using the unpaired Mann-Whitney test. Results are means ±SEM.

**P<0.01, significantly different between mice treated with hippurate and controls. †P< 0.05, ††P<0.01, significantly different between mice treated with benzoate and saline treated controls.

629
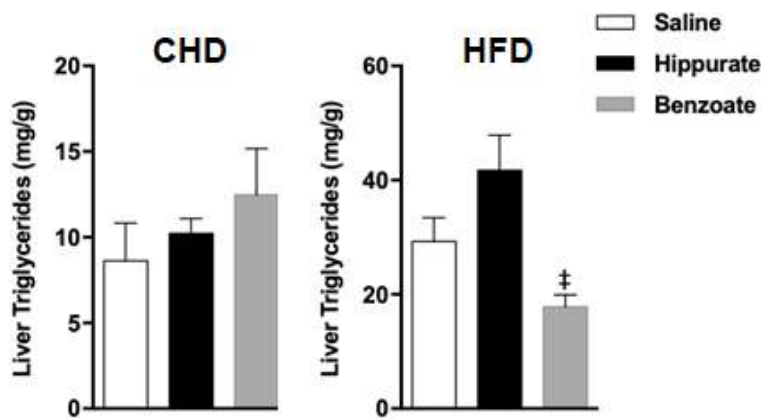
630

631 **Supplementary Figure 6. Effect of chronic administration of hippurate and benzoate**

632 **on liver triglycerides content in C57BL6/J mice.** The effect of chronic subcutaneous

633 administration of the metabolites (5.55mM) for 42 days on liver triglycerides was tested in

634 mice fed control chow diet (CHD) or high fat diet (HFD) for 56 days. Assay was carried out in

635 6 mice per group. Data were analyzed using the unpaired Mann-Whitney test.

636 Results are means ± SEM

637 ‡P<0.05, significantly different between mice treated with benzoate and hippurate.

638

639

640 **Supplementary Table S1**

641 Association between microbiota functional potential mapped to KEGG Orthologs (KOs)

642 database and urine hippurate levels.

643

644 **Supplementary Table S2**

645 Association between microbiota functional potential mapped to the eggNOG database and

646 urine hippurate levels.

647

648 **Supplementary Table S3**

649 Association between microbiota functional potential mapped to gut-specific metabolic

650 modules (GMMs) describing phenylpropanoid metabolism and urine hippurate levels.

651

652 **Supplementary Table S4**

653 Association between abundance of gut-specific metabolic modules (GMMs) describing

654 phenylpropanoid metabolism and gene richness.

655

656 **Supplementary Table S5**

657 Phenylpropanoid metabolism potential in metagenomic species, assessed by mapping to

658 GMMs significantly associated to urine hippurate levels.

659

660 **Supplementary Table S6**

661 Association between the microbiota composition profiled as metagenomic OTUs (mOTUs)

662 and urine hippurate levels.

663

664 **Supplementary Table S7**

665 pFDR from Spearman's rank-based correlations between GMMs describing

666 phenylpropanoid metabolism and gene richnessbioclinical variables using Storey's FDR

667 correction.

668

669 **Supplementary Table 8**

670 pFDR from Mann-Whitney U test for hippurate stratification in each bioclinical variable

671 between using Storey's FDR correction.

672

673

31

REFERENCES

1   Lynch SV, Pedersen O. The Human Intestinal Microbiome in Health and Disease. *N Engl J Med* 2016;**375**:2369–79. doi:10.1056/NEJMra1600266

2   Li J, Jia H, Cai X, *et al.* An integrated catalog of reference genes in the human gut microbiome. *Nat Biotechnol* 2014;**32**:834–41. doi:10.1038/nbt.2942

3   Qin J, Li R, Raes J, *et al.* A human gut microbial gene catalogue established by metagenomic sequencing. *Nature* 2010;**464**:59–65. doi:10.1038/nature08821

4   Le Chatelier E, Nielsen T, Qin J, *et al.* Richness of human gut microbiome correlates with metabolic markers. *Nature* 2013;**500**:541–6. doi:10.1038/nature12506

5   Cotillard A, Kennedy SP, Kong LC, *et al.* Dietary intervention impact on gut microbial gene richness. *Nature* 2013;**500**:585–8. doi:10.1038/nature12480

6   Nicholson JK, Holmes E, Wilson ID. Gut microorganisms, mammalian metabolism and personalized health care. *Nat Rev Microbiol* 2005;**3**:431–8. doi:10.1038/nrmicro1152

7   Dumas M-E. The microbial-mammalian metabolic axis: beyond simple metabolism. *Cell Metab* 2011;**13**:489–90. doi:10.1016/j.cmet.2011.04.005

8   Nicholson JK, Holmes E, Kinross J, *et al.* Host-gut microbiota metabolic interactions. *Science* 2012;**336**:1262–7. doi:10.1126/science.1223813

9   Neves AL, Chilloux J, Sarafian MH, *et al.* The microbiome and its pharmacological targets: therapeutic avenues in cardiometabolic diseases. *Curr Opin Pharmacol* 2015;**25**:36–44. doi:10.1016/j.coph.2015.09.013

10   Dumas M-E, Barton RH, Toye A, *et al.* Metabolic profiling reveals a contribution of gut microbiota to fatty liver phenotype in insulin-resistant mice. *Proc Natl Acad Sci USA* 2006;**103**:12511–6. doi:10.1073/pnas.0601056103

11   Holmes E, Loo RL, Stamler J, *et al.* Human metabolic phenotype diversity and its association with diet and blood pressure. *Nature* 2008;**453**:396–400. doi:10.1038/nature06882

12   Elliott P, Posma JM, Chan Q, *et al.* Urinary metabolic signatures of human adiposity. *Sci Transl Med* 2015;**7**:285ra62. doi:10.1126/scitranslmed.aaa5680

13   Pallister T, Jackson MA, Martin TC, *et al.* Untangling the relationship between diet and visceral fat mass through blood metabolomics and gut microbiome profiling. *Int J Obes (Lond)* 2017;**41**:1106–13. doi:10.1038/ijo.2017.70

14   Hoyles L, Fernández-Real JM, Federici M, *et al.* Molecular phenomics and metagenomics of hepatic steatosis in non-diabetic obese women. *Nat Med* 2018;**24**:1070–80. doi:10.1038/s41591-018-0061-3

15   Lees HJ, Swann JR, Wilson ID, *et al.* Hippurate: The Natural History of a Mammalian-Microbial Cometabolite. *J Proteome Res* 2013;**12**:1527–46. doi:10.1021/pr300900b

32

710 16 Dumas M-E, Wilder SP, Bihoreau M-T, *et al.* Direct quantitative trait locus mapping of
711   mammalian metabolic phenotypes in diabetic and normoglycemic rat models. *Nat*
712   *Genet* 2007;**39**:666–72. doi:10.1038/ng2026

713 17 Pallister T, Jackson MA, Martin TC, *et al.* Hippurate as a metabolomic marker of gut
714   microbiome diversity: Modulation by diet and relationship to metabolic syndrome.
715   *Scientific Reports* 2017;**7**:13670. doi:10.1038/s41598-017-13722-4

716 18 Pedersen HK, Gudmundsdottir V, Nielsen HB, *et al.* Human gut microbes impact host
717   serum metabolome and insulin sensitivity. *Nature* 2016;**535**:376–81.
718   doi:10.1038/nature18646

719 19 Forslund K, Hildebrand F, Nielsen T, *et al.* Disentangling type 2 diabetes and metformin
720   treatment signatures in the human gut microbiota. *Nature* 2015;**528**:262–6.
721   doi:10.1038/nature15766

722 20 Jørgensen T, Borch-Johnsen K, Thomsen TF, *et al.* A randomized non-pharmacological
723   intervention study for prevention of ischaemic heart disease: baseline results Inter99.
724   *Eur J Cardiovasc Prev Rehabil* 2003;**10**:377–86.
725   doi:10.1097/01.hjr.0000096541.30533.82

726 21 Levey AS, Stevens LA, Schmid CH, *et al.* A new equation to estimate glomerular
727   filtration rate. *Ann Intern Med* 2009;**150**:604–12.

728 22 Toft U, Kristoffersen L, Ladelund S, *et al.* Relative validity of a food frequency
729   questionnaire used in the Inter99 study. *Eur J Clin Nutr* 2008;**62**:1038–46.
730   doi:10.1038/sj.ejcn.1602815

731 23 Dona AC, Jiménez B, Schäfer H, *et al.* Precision high-throughput proton NMR
732   spectroscopy of human urine, serum, and plasma for large-scale metabolic
733   phenotyping. *Anal Chem* 2014;**86**:9887–94. doi:10.1021/ac5025039

734 24 Blaise BJ, Shintu L, Elena B, *et al.* Statistical recoupling prior to significance testing in
735   nuclear magnetic resonance based metabonomics. *Anal Chem* 2009;**81**:6242–51.
736   doi:10.1021/ac9007754

737 25 Dona AC, Kyriakides M, Scott F, *et al.* A guide to the identification of metabolites in
738   NMR-based metabonomics/metabolomics experiments. *Comput Struct Biotechnol J*
739   2016;**14**:135–53. doi:10.1016/j.csbj.2016.02.005

740 26 Vieira-Silva S, Falony G, Darzi Y, *et al.* Species-function relationships shape ecological
741   properties of the human gut microbiome. *Nat Microbiol* 2016;**1**:16088.
742   doi:10.1038/nmicrobiol.2016.88

743 27 Storey JD, Tibshirani R. Statistical significance for genomewide studies. *Proc Natl Acad*
744   *Sci USA* 2003;**100**:9440–5. doi:10.1073/pnas.1530509100

745 28 Dixon P. VEGAN, a package of R functions for community ecology. *Journal of*
746   *Vegetation Science* 2003;**14**:927–30. doi:10.1111/j.1654-1103.2003.tb02228.x

747 29 Cloarec O, Dumas ME, Trygg J, *et al.* Evaluation of the orthogonal projection on latent
748   structure model limitations caused by chemical shift variability and improved
749   visualization of biomarker changes in 1H NMR spectroscopic metabonomic studies.
750   *Anal Chem* 2005;**77**:517–26. doi:10.1021/ac048803i

751 30 Blaise BJ, Giacomotto J, Elena B, *et al.* Metabotyping of Caenorhabditis elegans
752   reveals latent phenotypes. *Proc Natl Acad Sci USA* 2007;**104**:19808–12.
753   doi:10.1073/pnas.0707393104

754 31 Brial F, Le Lay A, Hedjazi L, *et al.* Systems Genetics of Hepatic Metabolome Reveals
755   Octopamine as a Target for Non-Alcoholic Fatty Liver Disease Treatment. *Scientific*
756   *Reports* 2019;**9**:3656. doi:10.1038/s41598-019-40153-0

757 32 Phipps AN, Stewart J, WRIGHT B, *et al.* Effect of diet on the urinary excretion of
758   hippuric acid and other dietary-derived aromatics in rat. A complex interaction between
759   diet, gut microflora and substrate specificity. *Xenobiotica* 1998;**28**:527–37.
760   doi:10.1080/004982598239443

761 33 Backhed F, Ding H, Wang T, *et al.* The gut microbiota as an environmental factor that
762   regulates fat storage. *Proc Natl Acad Sci USA* 2004;**101**:15718–23.
763   doi:10.1073/pnas.0407076101

764 34 Bridle KR, Crawford DHG, Ramm GA. Identification and characterization of the hepatic
765   stellate cell transferrin receptor. *Am J Pathol* 2003;**162**:1661–7. doi:10.1016/S0002-
766   9440(10)64300-3

767 35 Shi J, Zhao J, Zhang X, *et al.* Activated hepatic stellate cells impair NK cell anti-fibrosis
768   capacity through a TGF-β-dependent emperipolesis in HBV cirrhotic patients. *Scientific*
769   *Reports* 2017;**7**:44544. doi:10.1038/srep44544

770 36 Aron-Wisnewsky J, Prifti E, Belda E, *et al.* Major microbiota dysbiosis in severe obesity:
771   fate after bariatric surgery. *Gut* 2019;**68**:70–82. doi:10.1136/gutjnl-2018-316103

772 37 Akira K, Masu S, Imachi M, *et al.* 1H NMR-based metabonomic analysis of urine from
773   young spontaneously hypertensive rats. *J Pharm Biomed Anal* 2008;**46**:550–6.
774   doi:10.1016/j.jpba.2007.11.017

775 38 Zhao L-C, Zhang X-D, Liao S-X, *et al.* A metabonomic comparison of urinary changes
776   in Zucker and GK rats. *J Biomed Biotechnol* 2010;**2010**:431894–6.
777   doi:10.1155/2010/431894

778 39 Pontoizeau C, Fearnside JF, Nayratil V, *et al.* Broad-Ranging Natural Metabotype
779   Variation Drives Physiological Plasticity in Healthy Control Inbred Rat Strains. *J*
780   *Proteome Res* 2011;**10**:1675–89. doi:10.1021/pr101000z

781 40 Bitner BF, Ray JD, Kener KB, *et al.* Common gut microbial metabolites of dietary
782   flavonoids exert potent protective activities in β-cells and skeletal muscle cells. *J Nutr*
783   *Biochem* 2018;**62**:95–107. doi:10.1016/j.jnutbio.2018.09.004

784 41 Dumas M-E, Rothwell AR, Hoyles L, *et al.* Microbial-Host Co-metabolites Are
785   Prodromal Markers Predicting Phenotypic Heterogeneity in Behavior, Obesity, and
786   Impaired Glucose Tolerance. *Cell Rep* 2017;**20**:136–48.
787   doi:10.1016/j.celrep.2017.06.039

788 42 Thaiss CA, Itav S, Rothschild D, *et al.* Persistent microbiome alterations modulate the
789   rate of post-dieting weight regain. *Nature* 2016;**540**:540–51. doi:10.1038/nature20796

790 43 Patterson AD, Turnbaugh PJ. Microbial determinants of biochemical individuality and
791   their impact on toxicology and pharmacology. *Cell Metab* 2014;**20**:761–8.
792   doi:10.1016/j.cmet.2014.07.002

793 44 Shoaie S, Ghaffari P, Kovatcheva-Datchary P, *et al.* Quantifying Diet-Induced Metabolic
794   Changes of the Human Gut Microbiome. *Cell Metab* 2015;**22**:320–31.
795   doi:10.1016/j.cmet.2015.07.001

796 45 Zeevi D, Korem T, Zmora N, *et al.* Personalized Nutrition by Prediction of Glycemic
797   Responses. *Cell* 2015;**163**:1079–94. doi:10.1016/j.cell.2015.11.001

Supplementary List: Module definitions

MC0001   phenylalanine degradation (cinnamate production)

cpd   [phenylalanine] [cinnamate, NH3]

K10775

ref   MetaCyc Pathway: trans-cinnamoyl-CoA biosynthesis

MC0002   chlorogenate degradation

cpd   [chlorogenate] [caffeate, quinate]

K06889 K09252

ref   MetaCyc Pathway: chlorogenic acid degradation   [1]

MC0003   caffeate respiration

cpd   [caffeate]   [hydrocaffeate]

bactNOG04579

ref   [2]

MC0004   cinnamate conversion

cpd   [cinnamate]   [3-(3-hydroxyphenyl)propanoate]

K10797

ref   KEGG Pathway: phenylalanine degradation

MC0005   coumarate degradation

cpd   [coumarate]   [hydroxybenzoate]

cpd   [ferulate]   [vanillate]

cpd   [caffeate]   [protocatechuate]

cpd   [cinnamate]   [benzoate]

K01904 bactNOG05057

K01692 K01715 K01782 K01825 K13767 K15016 bactNOG19280

K00141

ref   MetaCyc Pathway: 4-coumarate degradation (anaerobic)   [3]

MC0006   (hydroxy)benzoate degradation

cpd   [(hydroxy)benzoate]   [3-hydroxypimeloyl-CoA]

K04105,K04107,K04108,K04109 K04110 bactNOG00950

K04112,K04113,K04114,K04115 K19515,K19516

K07537

K07538

K07539

ref   MetaCyc Pathway: 4-coumarate degradation (anaerobic)   MetaCyc Pathway: benzoyl-CoA degradation II (anaerobic)   Kegg module: M00541

MC0007   ferulate degradation

cpd   [ferulate]   [vanillin]

K12508

K18383

ref   MetaCyc Pathway: ferulate degradation

MC0008   vanillate conversion

cpd   [vanillin, (O2)]   [protocatechuate]

bactNOG00059

K03862,K03863 K15066

ref   MetaCyc Pathway: superpathway of vanillin and vanillate degradation   Kegg Pathway: aminobenzoate degradation

MC0009   cinnamate degradation

cpd   [cinnamate]   [benzoyl-CoA]

bactNOG08521

actNOG07134

COG0277

bactNOG05297

ref   MetaCyc Pathway: trans-cinnamoyl-CoA biosynthesis   MetaCyc Pathway: benzoyl-CoA biosynthesis

MC0010   quinate degradation

cpd   [quinate]   [protocatechuate]

cpd   [shikimate]   [protocatechuate]

K05358 COG0169

K03785 K03786 K13832

K09483 K15652

ref   MetaCyc Pathway: quinate degradation I   MetaCyc Pathway: quinate degradation II [4]

MC0011   4-hydroxybenzoate conversion

cpd   [4-hydroxybenzoate, O2]   [protocatechuate]

K00481

ref   Kegg Pathway: benzoate degradation   [4]   [5]

MC0012   catechin degradation

cpd   [catechin]   [protocatechuate, phloroglucinol carboxylic acid]

bactNOG14887

ref   [6]

MC0013   3-hydroxybenzoate conversion

cpd   [3-hydroxybenzoate, O2]   [protocatechuate]

K19065

ref   Kegg Pathway: benzoate degradation

MC0014   benzoate conversion

cpd   [benzoate, O2] [4-hydroxybenzoate]

K07824

ref   Kegg Pathway: benzoate degradation

MC0015   benzoate degradation (aerobic)

cpd   [benzoate, O2] [catechol, CO2]

K05549,K05550,K05784

K05783

ref   Kegg module: M00551   MetaCyc Pathway: benzoate degradation I (aerobic)

MC0016   benzoate degradation (anaerobic)

cpd   [benzoyl-CoA]   [3-hydroxypimeloyl-CoA]

K04112,K04113,K04114,K04115 K19515,K19516

K19066

K07534

K07535

K07536

K04118

ref   MetaCyc Pathway: benzoyl-CoA degradation III (anaerobic)   Kegg module: M00540

MC0017   phenylalanine degradation

cpd   [phenylalanine, 2-oxoglutarate] [CO2, glutamate, benzoyl-CoA]

K00832 K00812 K00813 K11358 K00817

K04103

K00146 K00129

K01912

K18361

K18355,K18356,K18357,K18358,K18359

ref   MetaCyc Pathway: phenylacetate degradation II (anaerobic)   MetaCyc Pathway: L-phenylalanine degradation II (anaerobic)

MC0018   cellulose and hemicellulose degradation (cellulolosome)

cpd   [cellulose, hemicellulose]   [ferulate, polysaccharide, oligosaccharide]

K01181 K13465

K09252

bactNOG05428

ref   MetaCyc Pathway: cellulose and hemicellulose degradation (cellulolosome)

MC0019   feruloyl esterase (cellulolosome)

cpd   [cellulose, hemicellulose]   [ferulate]

K09252

ref   MetaCyc Pathway: cellulose and hemicellulose degradation (cellulolosome)   MC0018

MC0020   hippurate hydrolase

cpd   [hippurate]   [glycine, benzoate]

K01451

ref   [7]

References

1.   Couteau, D., McCartney, A. L., Gibson, G. R., Williamson, G. & Faulds, C. B. Isolation and characterization of human colonic bacteria able to hydrolyse chlorogenic acid. *J. Appl. Microbiol.* **90,** 873–881 (2001).
2.   Hess, V., González, J. M., Parthasarathy, A., Buckel, W. & Müller, V. Caffeate respiration in the acetogenic bacterium Acetobacterium woodii: a coenzyme A loop saves energy for caffeate activation. *Appl. Environ. Microbiol.* **79,** 1942–1947 (2013).
3.   Hirakawa, H., Schaefer, A. L., Greenberg, E. P. & Harwood, C. S. Anaerobic p-coumarate degradation by Rhodopseudomonas palustris and identification of CouR, a MarR repressor protein that binds p-coumaroyl coenzyme A. *J. Bacteriol.* **194,** 1960–1967 (2012).
4.   Brzostowicz, P. C., Reams, A. B., Clark, T. J. & Neidle, E. L. Transcriptional cross-regulation of the catechol and protocatechuate branches of the beta-ketoadipate pathway contributes to carbon source-dependent expression of the Acinetobacter sp. strain ADP1 pobA gene. *Appl. Environ.*

Microbiol. **69,** 1598–1606 (2003).

5. Gonthier, M.-P. *et al.* Metabolism of dietary procyanidins in rats. *Free Radic. Biol. Med.* **35,** 837–844 (2003).
6. Arunachalam, M., Mohan, N. & Mahadevan, A. Cloning of Acinetobacter calcoaceticus chromosomal region involved in catechin degradation. *Microbiol. Res.* **158,** 37–46 (2003).
7. Caner, V., Cokal, Y., Cetin, C., Sen, A. & Karagenc, N. The detection of hipO gene by real-time PCR in thermophilic Campylobacter spp. with very weak and negative reaction of hippurate hydrolysis. *Antonie Van Leeuwenhoek* **94,** 527–532 (2008).